A Novel Saline Infusion Sonohysterography-Based Strain Imaging Approach for Evaluation of Uterine Abnormalities In Vivo

Preliminary Results

Eenas A. Omari, MS, Tomy Varghese, PhD, Mark A. Kliewer, MD

In this article, we demonstrate the feasibility of saline infusion sonohysterography-based strain imaging for the determination of stiffness variations in uterine masses in vivo. Strain images are estimated using a 2-dimensional multilevel hybrid algorithm developed for sector array ultrasound transducers. Coarse displacements are initially estimated using envelope echo signals, followed by a guided finer displacement estimation using window lengths on the order of 6 wavelengths and 7 A-lines on radiofrequency data. Strain images are obtained by estimating displacement slopes using least squares estimation. In this prospective study, we show that stiffer masses such as fibroids appear darker or as regions with low strain on strain images and are thus clearly differentiated when compared to normal uterine tissue. A high strain boundary around stiffer masses referred to as a "halo" due to increased slipping or sliding of the mass during the applied deformation is also visualized. Uterine polyps, on the other hand, are visualized as masses that are brighter or regions with high strain when compared to the background myometrium, indicating the presence of a softer mass. Axial strain images provide additional new information that may supplement current clinical B-mode imaging used for the diagnosis of uterine abnormalities. Our results show the feasibility of improving clinical diagnosis based on strain imaging.

Key Words—fibroids; polyps; saline infusion sonohysterography; strain; strain imaging; uterine cancer

Received June 27, 2011, from the Departments of Medical Physics (E.A.O., T.V.), Electrical and Computer Engineering (E.A.O., T.V.), and Radiology (M.A.K.), University of Wisconsin–Madison, Madison, Wisconsin USA. Revision requested August 29, 2011. Revised manuscript accepted for publication October 16, 2011.

This work is funded in part by National Institutes of Health grants 5R21CA140939-03 and R01CA112192-S103.

Address correspondence to Tomy Varghese, PhD, Department of Medical Physics, University of Wisconsin–Madison, 1111 Highland Ave, 1159 WIMR, Madison, WI 53705 USA.

E-mail: tvarghese@wisc.edu

Abbreviations
2D, 2-dimensional

Approximately 70% of all gynecologic consultations are due to abnormal uterine bleeding.[1] Some of the major causes of dysfunctional uterine bleeding include benign conditions such as the presence of leiomyomas or fibroids, softer ingrowths such as endometrial polyps, and adenomyosis, a diffuse infiltration of softer tissue into the myometrium. Leiomymas are the most common gynecologic masses in premenopausal women.[2] Endometrial polyps have malignancy rates of 0.8% to 4.8% in postmenopausal women with abnormal uterine bleeding.[3] Other causes may be life threatening, such as the presence of malignancies, including endometrial and uterine cancer. Adenomyosis is characterized by the presence of heterotrophic endometrial glands and stroma in the myometrium with hyperplasia of the adjacent smooth muscle,[4] Leiomyomas (or fibroids) are made up of an excessive extracellular matrix relative to the surrounding uterine smooth muscle. It consists of collagen, proteoglycans, matrix metalloproteinases, and

transforming growth factor β.[5] Magnetic resonance imaging is recommended as the first-choice modality for exact evaluation of submucous myoma uterine ingrowths before advanced minimal invasive treatment of myomas but does not satisfy current diagnostic demands for detection of endometrial abnormalities.[6]

Sonography has been used for the evaluation of women with abnormal uterine bleeding. The two primary diagnostic sonographic techniques used are transvaginal sonography and saline infusion sonohysterography.[7] Transabdominal sonography was initially used but has shown poor results in differentiating between adenomyosis and leiomyomas.[8] In most cases, transvaginal sonography can detect the presence of uterine fibroids and fibroid characteristics, including volume, number, location, and position.[9] However, the mass may appear as an area of increased echogenicity bulging into the endometrial cavity with echogenicity similar to that of the myometrium. In addition, it is difficult to distinguish a leiomyoma from a blood clot or a polyp, and leiomyomas also may obscure the endometrium on imaging or cause an overestimation of endometrial thickness.[10] Transvaginal sonography may be used initially in the detection of endometrial polyps, which may appear as hyperechoic masses surrounded by a hypoechoic endometrium; however, it may be difficult to detect some polyps because they may appear as a diffusely thickened endometrium.[10] Nevertheless, polyps may be better visualized during saline infusion sonohysterography, in which the saline pushes apart the uterine cavity, and the polyps appear as smoothly margined focal lesions that protrude into the endometrial cavity. Saline infusion sonohysterography is also effective in distinguishing diffuse endometrial changes and focal intracavitary protuberances; however, it is limited in its ability to differentiate between endometrial hyperplasia (premalignant polyps) and endometrial carcinoma.[11]

Ultrasound strain imaging has been proposed as a new method for the diagnosis of masses that cause dysfunctional uterine bleeding.[12] In vitro uterine strain imaging has shown promising results for differentiation between normal uterine myometrial tissue and abnormalities such as leiomyomas and endometrial polyps. Leiomyomas appear as stiffer masses when compared to the surrounding normal myometrium on strain images and have also been characterized by a slipping artifact visualized as a bright band or "halo" around the mass. This halo was introduced as a result of signal decorrelation artifacts at the boundary due to mass slippage with the applied deformation. Because they are softer than the normal surrounding myometrium, endometrial polyps, on the other hand, are depicted as brighter masses on strain images.[12] Recently, magnetic resonance elastography has also been shown to be a feasible technique for studying the in vivo mechanical properties of uterine leiomyomas.[13]

It is important to have an accurate diagnosis of the type of uterine masses that cause the abnormal uterine bleeding because clinical treatment and management differ substantially. Most uterine leiomyomas are asymptomatic and therefore require no treatment.[14] Uterine fibroids generally regress after menopause, and it has been shown that the risk of developing fibroids decreases with the number of pregnancies.[15] Transcervical resection is considered the most optimal treatment for endometrial polyps, and infertile women who have them have an increased rate of fertility once they are removed. Transcervical resection is easy to perform, and minimal complications are associated with the procedure.[16] Surgical procedures used in the removal of polyps include dilation and curettage, hysteroscopic polypectomy, endometrial ablation, and hysterectomy. However, dilation and curettage is the least satisfactory procedure, and some women require follow-up surgery.[17] Polypectomy or the removal of polyps is effective for both premenopausal and postmenopausal women.[17] In the case of adenomyosis, hormonal treatments can be used to reduce symptoms but they do not eliminate the problem, and total hysterectomy remains the only permanent solution for debilitating adenomyosis.[18] Endometrial cancers are treated with staging laparotomy, total abdominal hysterectomy, and bilateral salpingo-oophorectomy.[19,20]

In this study, we investigated the potential of differentiating between different causes of abnormal uterine bleeding in both premenopausal and postmenopausal women in vivo using saline infusion sonohysterography-based strain imaging. The next section describes in vivo radiofrequency data acquisition during saline infusion sonohysterography. Local displacements are tracked using a multilevel hybrid 2-dimensional (2D) strain imaging algorithm developed for sector array ultrasound transducers.[21] The potential for using strain images of leiomyomas and polyps acquired in vivo for diagnosis is then discussed in the "Results" and "Discussion" sections.

Materials and Methods

Sonographic Radiofrequency Data Acquisition

Data acquisition for saline infusion sonohysterography-based strain imaging is performed on adult female patients in the radiology sonography suites of the University of Wisconsin–Madison Hospital and Clinics. The patients

recruited for the study had already been scheduled for clinical saline infusion sonohysterography. Patient consent for the research study was obtained before the procedure. The data acquisition protocol and research study were approved by the University of Wisconsin-Madison Institutional Review Board.

Clinical saline infusion sonohysterography is first performed on the patient following the appropriate clinical standard of care. The procedure is generally performed early in the menstrual cycle when the menstrual period has stopped or almost stopped but before ovulation. The patient is placed in the traditional lithotomy position, and a baseline transvaginal sonographic examination is performed. Subsequently, the transducer is removed; a sterile speculum is inserted into the vagina; and the external os of the cervix is brought into view. The cervix is cleansed with a povidone-iodine solution and then cannulated with a 28-cm 5F balloon catheter. Once inside the uterine cavity, the balloon is inflated with 2 to 3 mL of saline to fix the catheter in place. The speculum is then removed, and the endovaginal probe is reinserted beside the catheter. Under sonographic observation, the balloon is retracted so it does not occlude the internal cervical os. The balloon is positioned either within the endocervical canal or in the lower uterine segment. Then, 10 to 30 mL of warmed saline is hand injected through the catheter at a constant slow rate. Although not objectively modulated, this rate is approximately 0.5 to 0.75 mL/s. The distension of the uterine cavity is monitored to ensure that it is gradually increasing, despite concomitant loss of fluid through the fallopian tubes. Such a slow rate tends not to induce pain, and indeed, pain was not a limiting factor in any of the cases. The rate of injection is not varied systematically. Sagittal and coronal images of the distended endometrial cavity are then obtained.

Saline is then withdrawn from the uterine cavity through the catheter, and the ultrasound system is configured (placed in the research mode) to capture radiofrequency data loops. Saline is then reinfused, and ultrasonic radiofrequency data frames are recorded during the infusion procedure. Figure 1 presents a flowchart for the data acquisition procedure on the patient. At the end of the procedure, the catheter balloon is deflated and removed. The entire procedure takes about 30 to 60 minutes depending on insertion and securing of the catheter with the balloon inflated to avoid slipping or catheter movement. Radiofrequency data acquisition for research, however, takes only 5 to 10 minutes. Saline has to be withdrawn out of the uterine cavity, followed by a subsequent reinjection, to obtain sufficient deformation of the uterine cavity for strain imaging.

B-mode sonograms and radiofrequency data are acquired with a Sonoline Antares system (Siemens Medical Solutions, Inc, Mountain View, CA) using an EC9-4 transvaginal array transducer. The transducer is excited at a center frequency of 8 MHz, and the radiofrequency data are acquired at a sampling frequency of 40 MHz. A single transmit focus is used during the imaging process with dynamic focusing during receive. The maximum number of frames that the system can acquire during injection of the saline is stored (typically 150 frames) for offline processing. Fourteen patients provided informed consent and participated in the research study. The mean age of the patients scanned was 44 years. Among the 14 patients, no masses were seen in 7; however, 3 had a diagnosis of fibroids, and 2 each had a diagnosis of polyps and endometrial cancer, respectively, based on pathologic results. The B-mode images obtained during saline infusion sonohysterography were read and evaluated by a radiologist and taken into consideration when evaluating the saline infusion sonohysterography-based strain images. The next section describes the data processing performed to obtain the strain images.

Data Processing for Strain Estimation

We use a new hybrid 2D cross-correlation algorithm,[21] which uses multiple 1-dimensional cross-correlation processing steps to estimate local displacements, along with 2D surface fitting on a sector grid to obtain subsample displacement estimates. The predeformation and postdeformation radiofrequency data are determined from the radiofrequency data loop acquired during saline infusion sonohysterography. The first frame in the data loop is initially selected as the predeformation frame, with the postdeformation frame separated by a specified frame interval. A frame interval of 5 is used for the images shown in this ar-

Figure 1. Flowchart showing the different steps involved in performing saline infusion sonohysterography and data acquisition on patients.

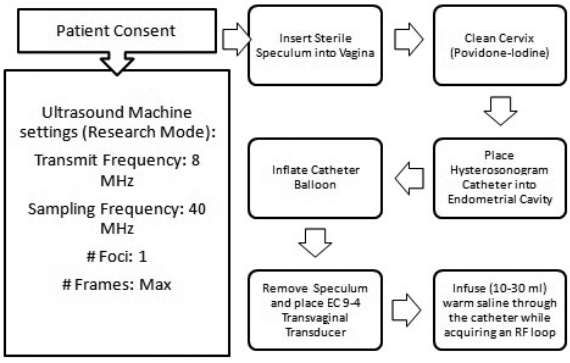

ticle. However, the frame interval can be increased if the deformation between the predeformation and postdeformation frames is too small to estimate local displacements and to compute the strain distribution. We use the deformation of the uterine wall induced by the saline injection during saline infusion sonohysterography as the mechanical stimulus for the strain imaging.

The strain estimation algorithm first estimates coarse displacements using the 1-dimensional normalized cross-correlation function on the predeformation and postdeformation envelope data frames. If the normalized correlation coefficient between the specified gated window and the corresponding neighboring gated A-line segment is lower than a threshold value, an interpolation step between the two neighboring radiofrequency segments of the postcompression data is performed, and the normalized cross-correlation function is recalculated as described by Chen and Varghese.[21] The peak of the cross-correlation function over several normalized cross-correlation functions in the 2D matrix is located, and a 2D surface fit with sector geometry is used to obtain subsample displacement estimates along the beam direction. The slope of the local displacements estimated in this manner is computed to obtain the strain distribution.

For all of the data processing described in this article, an overlap of 67% between rectangular gated windows is used with an 18-wavelength window length along the beam direction and 11 A-lines along the azimuthal direction; this procedure is done during the first processing step that uses envelope signals. Envelope signals are generated from the radiofrequency data using a Hilbert transform. The remainder of the processing is done with the radiofrequency echo signals to calculate accurate and precise displacements while progressively reducing the dimensions of the 2D processing window length along the beam direction and number of A-lines in the azimuthal direction. For the second processing step, a 75% overlap is used with a 12-wavelength window length along the beam direction and 11 A-lines along the azimuthal direction. The third and final processing step uses a 67% overlap with a 6-wavelength window length along the beam direction and 7 A-lines along the azimuthal direction.

Results

Figure 2 presents a B-mode image (Figure 2A) and the corresponding strain image (Figure 2B) estimated during saline infusion sonohysterography in a 50-year-old patient who later had a diagnosis of a fibroid based on the clinical sonographic examination. The red arrows on both the B-mode and strain images indicate the location of the fibroid within the uterine cavity. The yellow contours indicate the outer uterine wall. Clinical diagnosis is based on the radiologist's reading of the B-mode image loop obtained during the diagnostic saline infusion sonohysterographic procedure. The strain image provides a better definition of the fibroid, with a large strain boundary surrounding the fibroid, referred to as the halo, and a low strain region (darker) within the outline of the fibroid. The fibroid is outlined with the characteristic decorrelation halo that was also observed as a slipping artifact during the ex vivo imaging of fibroids previously described by Hobson et al.[12] Both the location and area of the fibroid highlighted along the edges are clearly visualized on the strain image in Figure 2B.

Figure 3A shows a B-mode image from a 46-year-old patient who had a diagnosis of a polyp based on diagnostic saline infusion sonohysterography, and the corresponding strain image is shown in Figure 3B. In a similar manner as described for Figure 2, the multilevel hybrid

Figure 2. B-mode image (**A**) obtained during saline infusion sonohysterography in a 50-year-old woman with a diagnosis of a submucosal fibroid and corresponding strain image (**B**). Red arrows indicate the location of the fibroid, and yellow contours indicate the location of the outer uterine wall.

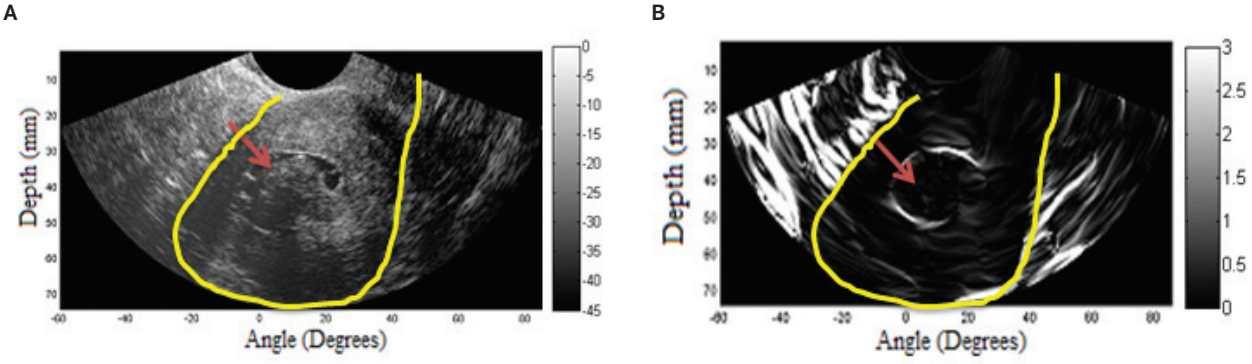

technique is used to estimate the local displacements and to generate the strain image (Figure 3B). The red arrows on the B-mode and strain images indicate the location of the uterine polyp. The strain image clearly shows the presence and location of the uterine polyp when compared to the B-mode image. This patient underwent a hysterectomy based on the clinical sonographic findings obtained during the saline infusion sonohysterographic procedure, and the pathology report was based on the excised uterus. The polyp appears to be brighter or as a region with higher strain when compared to the background myometrium, indicating that the polyp is softer than the surrounding tissue.

Figure 4A shows a B-mode image from a 61-year-old patient whose pathology report indicated the presence of endometrial cancer along with a fibroid. This patient also underwent a hysterectomy based on the clinical sonographic findings obtained during saline infusion sonohysterography, and the pathology report was based on the excised uterus. Observe that it is very difficult to visualize the cancer and fibroid on the B-mode image in Figure 4A. The uterine wall is outlined by the yellow contour on the B-mode image, and the red arrow indicates the region of interest. Note that on the strain image in Figure 4B, we see a highlighted region enclosing a stiffer region, indicating the location of the fibroid with the characteristic decorrelation halo. The region to the left of the fibroid is less uniform, which may be due to the presence of the diffuse endometrial cancer.

Finally, Figure 5A shows a B-mode image from a 44-year-old patient that does not indicate the presence of masses; however, after processing the radiofrequency data, the strain image in Figure 5B shows the possibility of the presence of a mass within the uterine cavity.

Discussion

The quality of the strain image obtained is dependent on the amount of deformation induced by the saline injection into the uterine cavity. If the amount of saline injected is too low, the deformation induced is too small to provide strain images with a reasonable signal-to-noise ratio. This situation has led to generation of suboptimal strain images in some instances because of the minimal deformation of the tissue. The amount of deformation applied via saline injection is dependent on the ability of the patient to tolerate the discomfort induced due to saline injection into the uterus; in other cases, insufficient deformation is due to the presence of saline from a previous infusion and the inability to withdraw sufficient fluid before starting a new infusion. Patient comfort is of paramount importance during the data acquisition because saline injection can be quite painful and distressing to the patient. Care should be taken to induce a sufficient deformation of the uterine wall that is tolerated by the patient to obtain high-quality strain images as well as having no saline or a minimum amount of it before starting the research data collection process.

In this article, we illustrate the application of saline infusion sonohysterography-based strain imaging to detect and image the variations in the stiffness of uterine masses in vivo. The results show a clear indication of the presence of masses in the uterine cavity when compared to the corresponding B-mode images. The fibroids appear darker on the strain images, whereas the polyps appear brighter because of the difference in stiffness between the mass and surrounding background myometrial tissue. We also show a case in which the B-mode image does not appear to differentiate any masses, but the strain image indicates the possible presence of a uterine mass. However, on the basis

Figure 3. B-mode image (**A**) obtained during saline infusion sonohysterography in a 46-year-old woman with a diagnosis of an endometrial polyp and corresponding strain image (**B**) obtained using the 2-dimensional multilevel hybrid algorithm. Red arrows indicate the location of the polyp, and yellow contours indicate the outer uterine wall.

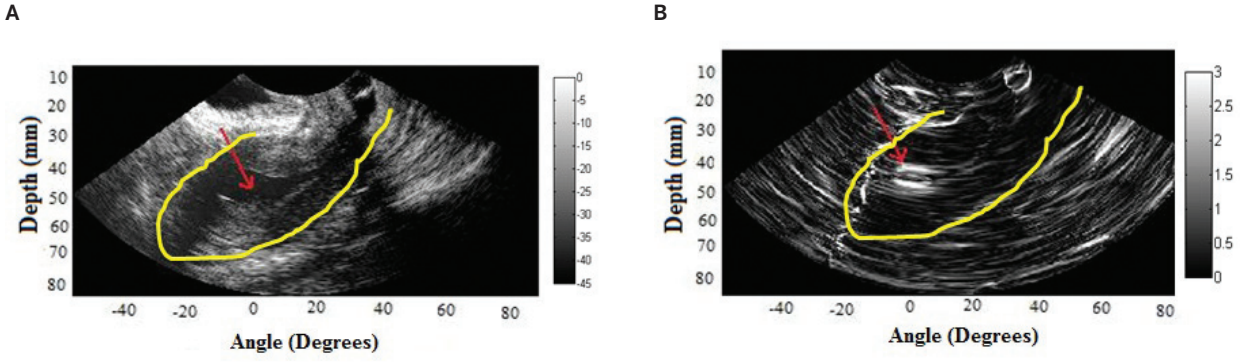

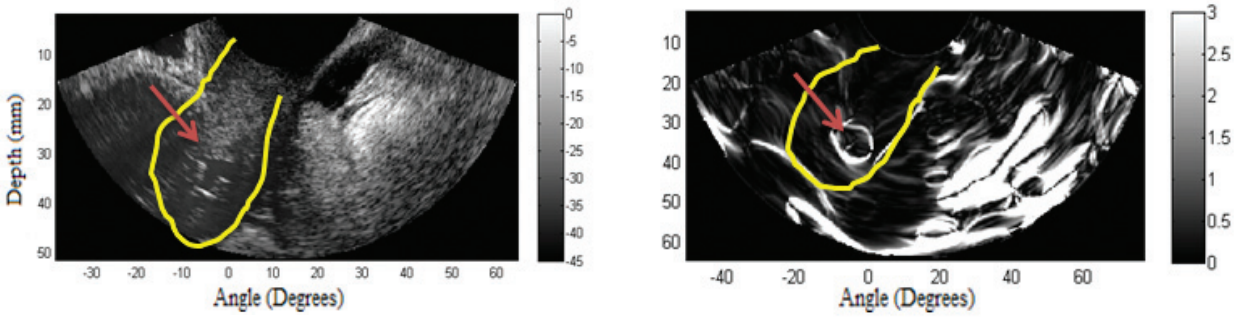

A B

Figure 4. B-mode image (**A**) obtained during saline infusion sonohysterography in a 61-year-old woman with a diagnosis of endometrial cancer and a fibroid based on the pathology report and corresponding strain image (**B**). Arrows indicate the region of interest, and yellow contours indicate the outer uterine wall.

of the limited data presented in this article, saline infusion sonohysterography-based strain imaging is expected to function only as a supplementary or adjunct imaging modality for characterization of focal uterine masses diagnosed on B-mode images. The use of saline infusion sonohysterography-based strain imaging as a stand-alone imaging technique for the detection of uterine masses requires additional validation on a larger number of patients and at multiple clinical sites.

Further investigation is also required to determine the in vivo contrast for different pathologic conditions. Color and spectral Doppler correlation in lesions of interest will be investigated in the future and might add value to the analysis. In this study, only a qualitative comparison of the underlying mass with the surrounding myometrial tissue was performed. Quantitative comparisons by solving the inverse problem or shear wave imaging approaches could be used in the future.[22,23]

Figure 5. B-mode image (**A**) obtained during saline infusion sonohysterography in a 44-year-old woman with a diagnosis of no apparent masses, where the yellow outline indicates the location of the uterus, and corresponding strain image (**B**), where the yellow arrow indicates the possible presence of a uterine mass.

A B

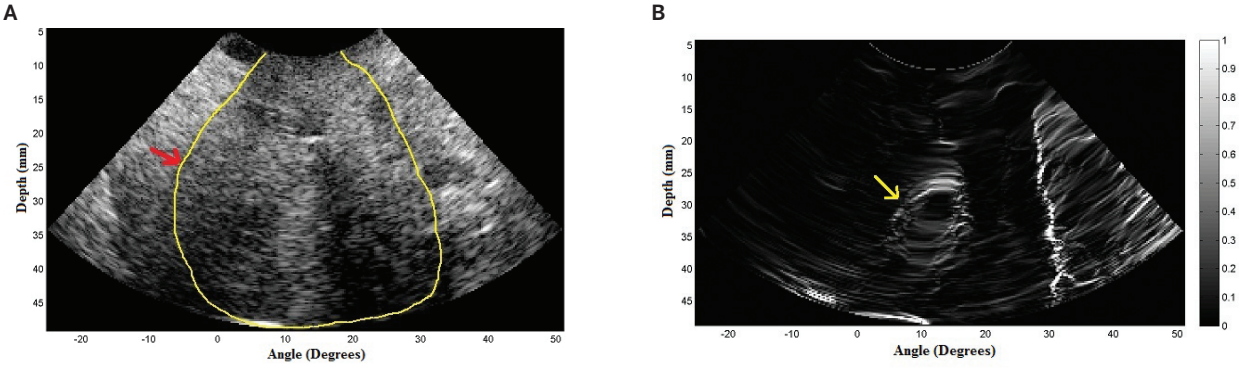

References

1. Spencer CP, Whitehead MI. Endometrial assessment re-visited. *Br J Obstet Gynaecol* 1999; 106:623–632.
2. Awonuga AO, Shavell VI, Imudia AN, Rotas M, Diamond MP, Puscheck EE. Pathogenesis of benign metastasizing leiomyoma: a review. *Obstet Gynecol Surv* 2010; 65:189–195.
3. Domingues AP, Lopes H, Dias I, De Oliveira CF. Endometrial polyps in postmenopausal women. *Acta Obstet Gynecol Scand* 2009; 88:618–620.
4. Gordts S, Brosens JJ, Fusi L, Benagiano G, Brosens I. Uterine adenomyosis: a need for uniform terminology and consensus classification. *Reprod Biomed Online* 2008; 17:244–248.
5. Malik M, Norian J, McCarthy-Keith D, Britten J, Catherino WH. Why leiomyomas are called fibroids: the central role of extracellular matrix in symptomatic women. *Semin Reprod Med* 2010; 28:169–179.
6. Dueholm M, Lundorf E, Olesen F. Imaging techniques for evaluation of the uterine cavity and endometrium in premenopausal patients before minimally invasive surgery. *Obstet Gynecol Surv* 2002; 57:388–403.
7. Okaro E, Condous G, Khalid A, et al. The use of ultrasound-based "soft markers" for the prediction of pelvic pathology in women with chronic pelvic pain: can we reduce the need for laparoscopy? *BJOG* 2006; 113:251–256.
8. Champaneria R, Abedin P, Daniels J, Balogun M, Khan KS. Ultrasound scan and magnetic resonance imaging for the diagnosis of adenomyosis: systematic review comparing test accuracy. *Acta Obstet Gynecol Scand* 2010; 89:1374–1384.
9. Lippman SA, Warner M, Samuels S, Olive D, Vercellini P, Eskenazi B. Uterine fibroids and gynecologic pain symptoms in a population-based study. *Fertil Steril* 2003; 80:1488–1494.
10. Davidson KG, Dubinsky TJ. Ultrasonographic evaluation of the endometrium in postmenopausal vaginal bleeding. *Radiol Clin North Am* 2003; 41:769–780.
11. Cohen, JR, Luxman D, Sagi J, Yovel I, Wolman I, David MP. Sonohysterography for distinguishing endometrial thickening from endometrial polyps in postmenopausal bleeding. *Ultrasound Obstet Gynecol* 1994; 4:227–230.
12. Hobson MA, Kiss MZ, Varghese T, et al. In vitro uterine strain imaging: preliminary results. *J Ultrasound Med* 2007; 26:899–908.
13. Stewart EA, Taran FA, Chen J, et al. Magnetic resonance elastography of uterine leiomyomas: a feasibility study. *Fertil Steril* 2011; 95:281–284.
14. Hutchins FL Jr. Uterine fibroids: diagnosis and indications for treatment. *Obstet Gynecol Clin North Am* 1995; 22:659–665.
15. Vollenhoven BJ, Lawrence S, Healy DL. Uterine fibroids: a clinical review. *Br J Obstet Gynaecol* 1990; 97:285–298.
16. Lieng M, Istre O, Qvigstad E. Treatment of endometrial polyps: a systematic review. *Acta Obstet Gynecol Scand* 2010; 89:992–1002.
17. Tjarks M, Van Voorhis BJ. Treatment of endometrial polyps. *Obstet Gynecol* 2000; 96:886–889.
18. Imaoka I, Wada A, Matsuo M, Yoshida M, Kitagaki H, Sugimura K. MR Imaging of disorders associated with female infertility: use in diagnosis, treatment, and management. *Radiographics* 2003; 23:1401–1421.
19. Kim YB, Holschneider CH, Ghosh K, Nieberg RK, Montz FJ. Progestin alone as primary treatment of endometrial carcinoma in premenopausal women: report of seven cases and review of the literature. *Cancer* 1997; 79:320–327.
20. Ramirez PT, Frumovitz M, Bodurka DC, Sun CC, Levenback C. Hormonal therapy for the management of grade 1 endometrial adenocarcinoma: a literature review. Gynecol Oncol 2004; 95:133–138.
21. Chen H, Varghese T. Multilevel hybrid 2D strain imaging algorithm for ultrasound sector/phased arrays. *Med Phys* 2009; 36:2098–2106.
22. Jiang J, Brace C, Andreano A, et al. Ultrasound-based relative elastic modulus imaging for visualizing thermal ablation zones in a porcine model. *Phys Med Biol* 2010; 55:2281–2306.
23. DeWall RJ, Varghese T, Madsen EL. Shear wave velocity imaging using transient electrode perturbation: phantom and ex vivo validation. *IEEE Trans Med Imaging* 2011; 30:666–678.